


Physically entrapped gelatin in polyethylene glycol scaffolds for three-dimensional chondrocyte culture

Journal of Bioactive and
Compatible Polymers
2016, Vol. 31(5) 513–530
© The Author(s) 2016
Reprints and permissions:
sagepub.co.uk/journalsPermissions.nav
DOI: 10.1177/0883911516633893
jbc.sagepub.com


Jingjing Zhang¹, Ayeesha Mujeeb¹,
Junxia Feng¹, Yijiang Li¹, Yanan Du^{2,3},
Jianhao Lin⁴ and Zigang Ge^{1,4}

Abstract

Developing tissue-engineered constructs for clinical use must satisfy the fundamental biologic parameters of biocompatibility, cell adhesiveness, and biodegradability. Physical entrapment of bioactive agents into synthetic polymers, as three-dimensional scaffolds, holds great promise for cell culture applications. Here, in an attempt to elucidate the effects of physical interlocking of natural and synthetic gel networks on cell responses within three-dimensional microenvironments, gelatin (of different concentrations) was physically incorporated into macroporous polyethylene glycol (PEG) hydrogels to fabricate PEG-GEL1 (10:1, PEG:gelatin) and PEG-GEL5 (10:5, PEG:gelatin). The effect of the physically entrapped gelatin on primary chondrocytes was investigated in relation to cell distribution, morphology and viability, proliferation, gene expression, and extracellular matrix accumulation *in vitro*. Our findings have shown successful incorporation of two different concentrations of gelatin into polyethylene glycol macroporous hydrogels through physical mixing. These physical blends not only enhanced chondrocyte adhesion and proliferation but also boosted gene expression of collagen II and aggrecan after 14 days in culture. Although results demonstrated that gelatin levels dropped sharply in PEG-GEL1 and PEG-GEL5 in the first 7 days, however evidently, after days 14 and 21 gelatin levels in both groups remained substantially unchanged and in turn enhanced glycosaminoglycan formation *in vitro*. Thus, the modification of

¹Department of Biomedical Engineering, College of Engineering, Peking University, Beijing, People's Republic of China

²Department of Biomedical Engineering, Tsinghua University, Beijing, People's Republic of China

³Collaborative Innovation Center for Diagnosis and Treatment of Infectious Diseases, Hangzhou, People's Republic of China

⁴Arthritis Clinic & Research Center, Peking University People's Hospital, Beijing, People's Republic of China

Corresponding author:

Zigang Ge, Department of Biomedical Engineering, College of Engineering, Peking University, Beijing 100871, People's Republic of China.

Email: gez@pku.edu.cn

polyethylene-glycol-based scaffolds with physically entrapped gelatin may be sufficient for dictating three-dimensional microenvironments for chondrocyte cultures.

Keywords

Cell adhesion, gelatin, physical entrapment, macroporous hydrogels, chondrocyte culture

Introduction

Biomaterials have been extensively used as scaffolds in regenerative medicine, enhancing the delivery of cells and molecules,¹ while guiding de novo tissue organization^{2,3} and stem-cell-lineage differentiation.⁴ Biomaterials possess properties that have a significant effect on cell behavior, such as pore structure,⁵⁻⁷ topography,⁸ and chemical motifs.⁹ For decades, bioengineers tested numerous synthetic materials for cell culture applications that primarily lacked bioactivity and led to cell toxicity in vitro. To overcome this problem, synthetic materials were decorated with natural polymers or bioactive molecules to optimize microenvironments for cell functions in vitro.^{10,11}

Both chemical and physical modifications of synthetic polymers have been extensively explored, using gelatin (a by-product of collagen hydrolysis) as an illustrative example. Chemical modifications or cross-links are permanent bonds formed by covalent interactions, whereas physical cross-links are due to non-covalent interactions such as hydrogen bonding, hydrophobic interactions, and ionic bonds. As the physical cross-links are not permanent in nature, these cross-links are sufficient to hold the networks of fibers together for cell encapsulation under cell culture conditions. For instance, interpenetrating networks of gelatin methacrylamide (GelMA) and polyethylene glycol (PEG) have shown great potential for supporting internal endothelial cell encapsulation.¹² On the contrary, gelatin chemically cross-linked to PEG and poly ϵ -caprolactone (PCL) hydrogels, through glutaraldehyde or genipin cross-linking agents has shown some promising results.^{12,13} Additionally, an enzyme-catalyzed gelatin cross-linking method was also developed for cell encapsulation.^{14,15} These types of chemical cross-linking procedures have brought disadvantageous effects on cellular functions and subsequent mechanical properties of scaffolds in vitro.^{16,17}

Physical entrapment is one of the methods for introducing biomolecules onto materials with well-defined properties that do not rely on chemical processing. Gelatin is produced by partial hydrolysis of collagen and is one of the most widely used biomolecule due to its relatively low antigenicity and excellent bioactivity.^{10,13} Gelatin is usually incorporated through glutaraldehyde or genipin cross-linking.^{12,13} However, this cross-linking process is often harmful and leads to cell toxicity.¹⁷ Physical entrapment is an effective way of treating inert materials. Biomolecules such as collagen, fibronectin, laminin, and peptides have been physically incorporated into polymeric matrices to promote cell adhesion.¹⁸ In another illustrative study, non-chemically modified gelatin into degradable synthetic polyvinyl alcohol/tyramine (PVA-Tyr) hydrogels enhanced cell adhesion and proliferation under cell culture conditions.^{19,20}

Herein, we employed PEG as a platform to investigate the physical incorporation of gelatin into macroporous hydrogels, which were subjected to three-dimensional (3D) chondrocyte culture in vitro. Engineered microenvironments have the ability to control cellular functions, via the use of biochemical and physical cues.²¹ Therefore, systematically, by selecting two different gradients of gelatin, the following PEG-gelatin hydrogels were prepared: PEG-GEL1 (10:1 w/w, PEG:gelatin) and PEG-GEL5 (10:5 w/w, PEG:gelatin), respectively. Next, the effect of

physically entrapped gelatin (within the scaffold) on chondrocyte behavior, particularly cell adhesion and viability, proliferation, gene expression, and extracellular matrix (ECM) deposition *in vitro*, was assessed. Research findings from this study also provide insights into designing physical blends as 3D scaffolds that are stable and reliable for cell culture applications *in vitro*.

Materials and methods

Synthesis of poly (ethylene glycol) diacrylate oligomer

Poly (ethylene glycol) diacrylate (PEGDA) oligomer was synthesized according to a previously reported method.²² Dry PEG powder (5 g, 4 kDa; Sigma, USA) was suspended in 80 mL of anhydrous dichloromethane (DCM; Beijing Tongguang Fine Chemicals, People's Republic of China). A solution containing 1.06 mL of triethylamine (99.7%; Acros Organic, USA) and 1.26 mL of acryloyl chloride triethylamine was added to the reaction mixture drop wise and left overnight in liquid-nitrogen-maintained atmospheric temperatures. At room temperature, after washing with 2 M K₂CO₃ solution, the mixture was precipitated in cold diethyl ether and freeze dried at -58°C for 48 h to obtain lyophilized PEGDA powder.

Preparation of physically entrapped gelatin-PEG scaffolds

The precursor mixture was prepared by dissolving PEGDA (10% w/v) in saturated NaCl solution and was further mixed with NaCl crystals (450 mg mL⁻¹, with a diameter ranging between 80 and 150 μm) at room temperature. Ammonium persulphate (APS, 0.2 w/v, 25 μL; Ameresco, People's Republic of China) and N,N,N',N'-tetramethylethylenediamine (TEMED, 0.5 w/v, 25 μL; Sigma, People's Republic of China) were added to cross-link the precursor mixture to fabricate macroporous hydrogels. Hydrogels were immersed in deionized water (DIW) for 48 h before replacing DIW eight times to remove the unreacted precursor and NaCl. The resultant hydrogels were frozen and lyophilized before further use. For physical entrapment of gelatin into PEG hydrogels, gelatin powder (G9382; Sigma, People's Republic of China) and PEGDA were dissolved into saturated NaCl solution. During the preparation of gelatin-PEG mix, the mixture was incubated in the water bath at 60°C for 2 h in order to dissolve gelatin and form a homogeneous mixture. PEG macroporous hydrogels containing the following molar ratios of gelatin were prepared: PEG-GEL1 (10:1 w/w, PEG:gelatin) and PEG-GEL5 (10:5 w/w, PEG:gelatin), respectively. Arg-Glu-Asp (RED) peptides were modified to PEG scaffolds to prepare PEG-RED scaffolds which served as the control group.

Scanning electron microscopy and swelling ratio

The macroporous structure of the hydrogels was investigated using scanning electron microscopy (SEM, Quanta 200 FEG; FEI, USA) at an accelerating voltage of 5 kV. Samples were mounted on a metal stub and sputter-coated with gold palladium for 80 s at 18 mA.

The swelling ratio was measured using the method described by Nair et al.²³ After the weight of the freeze-dried hydrogels was measured, the samples were immersed in phosphate-buffered saline (PBS) at 37°C for 2 h. Excess water was then removed using a filter paper, and the weights of the swollen macroporous hydrogels were recorded, where $n = 3$. The swelling ratio % (SR) was calculated using the following formula: $SR = [(W_s - W_d) / W_d] \times 100\%$, where W_d and W_s are the weight of the dried and swollen hydrogels, respectively.

Weight loss analysis, ninhydrin staining, and quantification of gelatin in PEG scaffolds

Degradation studies were performed using the method previously described.²⁴ Lyophilized macroporous samples ($4 \times 2.5 \times 1 \text{ mm}^3$) were immersed in PBS (2 mL) at pH 7.4 (mass to volume ratio > 10) and incubated at 37°C. The solution was changed every 3 days. Analysis was carried out at Days 0, 7, 14, and 21 *in vitro*. The following formula was used to calculate the percentage of weight loss (% WL) of the hydrogels: Percentage of weight loss (% WL) = $[(W_i - W_f) / W_i] \times 100\%$, where W_i and W_f are the initial weight of the dried hydrogels and the weight of the hydrogels after incubation in PBS, respectively.

Gelatin integration within the PEG scaffolds was evaluated by ninhydrin staining.²⁵ In brief, ninhydrin/ethanol solution (1M, 20 μL) was added drop wise onto the hydrogels, before transferring samples into a tube, which was incubated at 80°C for 10 min in the water bath. Subsequently, hydrogels were removed and photographed with a Sony digital camera (DSC-H200). The shape and size of the samples were measured using a caliper ruler.

Furthermore, the amount of gelatin remained within the 3D hydrogels was quantified using Pierce™ BCA Protein Assay Kit (Thermo Scientific, China) according to the manufacturer's instructions. At each time interval, PEG-GEL hydrogels were bisected into small pieces and incubated in PBS at 56°C in order to release the entrapped gelatin. Next, sample supernatant (2 μL) was mixed in PBS (18 μL) and incubated with 200 μL BCA working solution (BCA solution A:BCA solution B = 50:1, v/v) at 37°C for 30 min. The absorbance densities were obtained at 570 nm. The amount of gelatin was determined using a standard curve of known gelatin content. The assay was performed in triplicates, where $n = 3$. Percentage of gelatin (%) = $[W_g / W_s] \times 100\%$, where W_g and W_s represent the weight of the gelatin remained in the hydrogel and the weight of the entire hydrogel, respectively.

Chondrocyte culture and cell distribution

Chondrocytes were isolated from the knee joints of pigs (Yorkshire, 10–12 months). Articular cartilage was excised and digested in 0.15% collagenase II (Sigma, People's Republic of China) for 12 h with intermittent rotation. The harvested chondrocytes were cultured in Dulbecco's modified Eagle's medium (DMEM, 12800017; Gibco-Invitrogen, People's Republic of China) containing 10% fetal bovine serum, 100 $\mu\text{g mL}^{-1}$ streptomycin, and 100 $\mu\text{g mL}^{-1}$ penicillin. When a sub-confluent cell layer was observed in cell culture flasks, cells were trypsinized using 0.05% trypsin-0.53 mM ethylenediaminetetraacetic acid tetrasodium salt (EDTA.4Na) (Gibco-Invitrogen). The cell pellet was re-suspended in fresh culture medium to adjust the required cell concentration before cell seeding. Prior to 3D cell culture, hydrogels ($4 \times 2.5 \times 1 \text{ mm}^3$) were immersed in 75% ethanol for 4 h and washed with PBS before cell seeding. A 1 mL of medium with suspended chondrocytes (3×10^5 cells per well) at passage 2 was added. The culture medium was changed every 3 days to aid cell growth. Chondrocyte distribution was observed under the optical microscope at 0, 4, and 24 h.

Fluorescence labeling of encapsulated chondrocytes in PEG-gelatin scaffolds

Chondrocytes adhered to the scaffolds ($4 \times 2.5 \times 1 \text{ mm}^3$) at Day 3 were incubated in 5(6)-carboxy-fluorescein diacetate N-succinimidyl ester (CFDA-SE) (21888; Sigma, People's Republic of China) solution (5 μM , 100 μL) for 20 min. Samples were rinsed with PBS and then immersed in isothiocyanate rhodamine B (R1755-RBITC; Sigma, People's Republic of China) solution at a

concentration of 0.1 mg mL^{-1} for 24 h at 4°C in order to stain physically entrapped gelatin within the PEG hydrogels.²⁶ After 24 h, samples were washed with PBS three times to remove excess RBITC. Samples were observed under the confocal laser scanning microscopy (CLSM-LSM510; Zeiss, Germany). The RBITC-labeled hydrogels were viewed at an emission wavelength of 580 nm and an excitation wavelength of 543 nm. Whereas, CFDA-SE-labeled chondrocytes were viewed at an emission wavelength was 530 nm and the excitation wavelength was 490 nm, respectively.

F-actin and integrin $\beta 1$ staining, and western blot

Chondrocytes were seeded into hydrogels ($4 \times 2.5 \times 1 \text{ mm}^3$) and cultured for 3 days. For F-actin staining, samples were fixed with 4% paraformaldehyde, and chondrocytes were permeabilized in 0.1% Triton X-100, stained with rhodamine phalloidin (PHDR1, cytoskeleton) for 30 min, followed by nuclear counter staining with 4,6-diamidino-2-phenylindole (DAPI; Sigma, USA) for 2 h. The stained samples were observed under the CLSM (LSM510; Zeiss), and ImageJ software was used to measure the area of cell aggregates, aspect ratio, and subsequent roundness.

After 3 days in culture, the constructs ($4 \times 2.5 \times 1 \text{ mm}^3$) were fixed in paraformaldehyde solution (4% v/v, pH7.4), dehydrated, and embedded in paraffin. The samples were sectioned at a thickness of $5 \mu\text{m}$ for further staining. For immunocytochemistry staining of integrin $\beta 1$, the sections were permeabilized in 0.5% Triton X-100 for 15 min and blocked with 5% bovine serum albumin (BSA) for 30 min before washing twice with PBS. Next, samples were incubated with rabbit anti-integrin $\beta 1$ polyclonal antibody (1:100 sc-8978; Santa Cruz Biotechnology, Inc., Germany) for 1 h. To remove the non-bound primary antibody, samples were washed three times with PBS. Subsequently, secondary antibody (1:500 donkey anti-rabbit IgG-Alexa Fluor[®]-488, bs-0295d-af488; Bioss, People's Republic of China) was added for 1 h in the dark. To remove the non-bound secondary antibody, samples were washed five times with PBS. Samples were mounted on the glass slides with DAPI, and images were captured using a confocal microscope.

Chondrocytes were seeded into macroporous hydrogels ($4 \times 2.5 \times 1 \text{ mm}^3$) and cultured for 3 days. Chondrocytes after 3 days in culture were lysed in RIPA lysis buffer (R0020; Solarbio) with fresh protease inhibitor of 0.1% phenylmethanesulfonyl fluoride (PMSF; Solarbio, People's Republic of China). Total cell lysate was boiled after mixing with $4\times$ sodium dodecyl sulfonate (SDS) loading buffer (P1015; Solarbio, People's Republic of China). Western blotting was performed according to the manufacturers' protocol. Rabbit anti-integrin $\beta 1$ polyclonal antibodies (dilution 1:100, sc-8978; Santa Cruz Biotechnology, Europe) were combined with horseradish peroxidase (HRP) linked antibody rabbit IgG (7074, Cell Signaling). The complex of the antigen and the antibody was illuminated by chemiluminescence and detected by ChemiDoc X-ray spectrometer (XRS)+Molecular Imager (Bio-Rad, USA) and then quantified by Quantity One image software (Bio-Rad).

Cell viability and proliferation

Chondrocytes were seeded into macroporous hydrogels ($4 \times 2.5 \times 1 \text{ mm}^3$). MTT assay 3-(4,5-dimethyl-2-thiazolyl)-2,5-diphenyl-2H-tetrazolium bromide (M2128; Sigma, People's Republic of China) was used to test cell viability. After culturing for 1, 4, and 7 days, cells were mixed with $200 \mu\text{L}$ of MTT solution and incubated for 3 h. Then, dimethyl sulfoxide (DMSO) was added and the absorbance was detected at 570 nm in a microplate reader ($n=4$, Synergy; BioTek, USA). After 7 and 14 days in culture, cell viability was observed via fluorescein diacetate (FDA, F7378; Sigma, People's Republic of China) and propidium iodide (PI, P4170; Sigma, People's Republic of China) staining. The FDA ($100 \mu\text{L}$, $2 \mu\text{g mL}^{-1}$) solution was added on top of each sample. Samples were

then incubated for 15 min in an incubator at 37°C. The staining solution was removed, and the samples were washed with PBS three times. Next, PI (100 μL , 5 $\mu\text{g mL}^{-1}$) was added. Samples were then washed with PBS three times for 5 min. The hydrogels were viewed under the confocal microscope at an excitation wavelength of 488 nm (green) and 535 nm (red). Cell numbers were assessed with Hoechst 33258 dye (H6024; Sigma, People's Republic of China). After 14 days in culture, chondrocytes in each well were lysed with 100 μL sterile distilled water, and the dissolved solution was transferred into 96-well plates. H33258 solution (100 μL , 0.1 $\mu\text{g mL}^{-1}$) was added to each well, and readings were recorded in triplicates (where $n=3$) using a microplate reader (CEMINI XS, Molecular Devices). The fluorescence was recorded at an excitation wavelength of 360 nm and emission wavelength of 465 nm, respectively.

DMMB assay for glycosaminoglycan quantification

Chondrocytes at passage 2 were seeded into macroporous hydrogels ($4 \times 2.5 \times 1 \text{ mm}^3$) and cultured for 7 and 14 days, before the constructs were digested with proteinase K (50 $\mu\text{g mL}^{-1}$) at 56°C overnight and examined with 1,9-dimethylmethylene blue (DMMB, 341088; Sigma, People's Republic of China). The solution was vortexed for 30 min and then centrifuged at $10,000 \times g$ for 10 min. The centrifugal deposits were dissolved in a decomplexation solution, and absorbance was recorded at 630 nm. The standard curve of sulfated glycosaminoglycan (sGAG) content was recorded with chondroitin sulfate (27042-10G-F; Sigma, People's Republic of China). The assay was performed in triplicates, where $n=3$.

Quantitative gene expression by RT-PCR

The chondrocytes at passage 2 were seeded into macroporous hydrogels ($4 \times 2.5 \times 1 \text{ mm}^3$). At Day 14, cells were lysed in 1 mL Trizol (15596-026; Invitrogen, People's Republic of China) for 5 min, and the extraction process of the RNA was carried out according to the manufacturer's instructions. The cDNA was synthesized by following the instructions of the iScript™ cDNA synthesis kit (Bio-Rad) after detecting the RNA concentration with the Nano-Drop (NanoDrop Technologies, USA). The Power SYBR Green PCR Master Mix (Applied Biosystem, USA) was used in this PCR system, and the experiment was conducted on the Applied Biosystem 7500 Real-Time PCR System (Applied Biosystem) at 95°C for 15 min, followed by 40 cycles of 15-s denaturation at 94°C, 30-s annealing at 55°C, and 30-s elongation at 72°C. The target genes were normalized by the reference gene glyceraldehydes-3-phosphate dehydrogenase (GAPDH). The primers used in this experiment are listed in Table 1.

Statistical analysis

Analysis was performed using SPSS V17.0 (one-way analysis of variance (ANOVA), Least-significant difference (LSD), $p < 0.05$). The data are expressed as mean \pm standard deviation with significant p values, * $p < 0.05$; ** $p < 0.01$; *** $p < 0.001$.

Results

Characterization of macroporous PEG-gelatin scaffolds

In this study, hydrogels consisted of conventional interconnected pores with average pore diameters ranging between 80 and 200 μm (Figure 1(a) and (b)). Gelatin incorporation had no significant effect on the microporous morphologies. In addition, inhomogeneous integration of gelatin into 3D

Table 1. Primer sequences for chondrogenic marker genes.

Target primer	Sequence forward and reverse (from 5' to 3')
<i>GAPDH</i>	ATGGTGAAGGTCGGAGTGAA; AATGAAGGGGTCATTGATGG
<i>Aggrecan</i>	CATCACCGAGGGTGAAGC; CCAGGGGCAAATGTAAAGG
<i>Collagen I</i>	CAGAACGGCCTCAGGTACCA; CAGATCACGTCATCGCACAAAC
<i>Collagen II</i>	TGAGAGGTCTTCCTGGCAAA; GAAGTCCCTGGAAGCCAGAT
<i>Collagen X</i>	TGCTGCTGCTATTGTCCTTG; TGAAGAACTGTGCCTTGGTG
<i>Sox-9</i>	ATCAGTACCCGCACCTGCAC; CTTGTAATCCGGGTGGTCCTT

gel constructs was observed (Figure 1(c)). Gelatin integration had no significant effect on the swelling properties of the hydrogels, and the value recorded was 12 (Figure 1(d)).

Scaffold degradation

Relatively uniform pore morphology was observed in all hydrogels before degradation (Figure 2(a)). After 21 days of degradation, no significant morphological changes were observed microscopically, and PEG-GEL1 and PEG-GEL5 revealed similar structural properties (Figure 2(a)). The weight loss of each sample was also recorded (Figure 2(b)). In comparison with PEG-RED, a visible weight loss was observed in PEG-GEL1 and PEG-GEL5 groups after 21 days of immersion in PBS. Statistically, the weight loss of PEG-GEL5 was evidently higher than PEG-GEL1 *in vitro*.

Quantification of gelatin in PEG scaffolds

Gelatin concentrations in macroporous PEG hydrogels before and after degradation were examined (Figure 3). Photographs revealed uniform distribution of gelatin within the polymeric networks of PEG-GEL1 (in pink) and PEG-GEL5 (in purple) before degradation (Figure 3(b,c)). However, a drastic color change from purple to light pink was observed in PEG-GEL5 after 21 days *in vitro*, indicating a significant reduction in gelatin composition (Figure 3(c,f)).

Again, the amount of gelatin in macroporous PEG hydrogels was further quantified by Pierce BCA Protein assay (Figure 3(g)). Sharp drops in gelatin levels were observed between Days 0 and 7, from $7.9\% \pm 1.6\%$ to $3.11\% \pm 0.37\%$ and $15.26\% \pm 1.6\%$ to $13.42\% \pm 0.42\%$ in PEG-GEL1 and PEG-GEL5 hydrogels. Interestingly, between Days 7 and 21, gelatin compositions remained substantially unchanged in both groups, PEG-GEL1 (~3% gelatin) and PEG-GEL5 (~13% gelatin). As shown, statistically, gelatin compositions in PEG-GEL1 and PEG-GEL5 groups varied significantly at Day 7 ($p < 0.01$), Day 14 ($p < 0.001$), and Day 21 ($p < 0.001$).

Distribution and morphology of chondrocytes in 3D

To investigate the potential role of PEG-gelatin hydrogels as bioactive scaffolds, chondrocytes were seeded and cultured *in vitro*. Upon seeding, cells instantly formed loose clusters after 4h

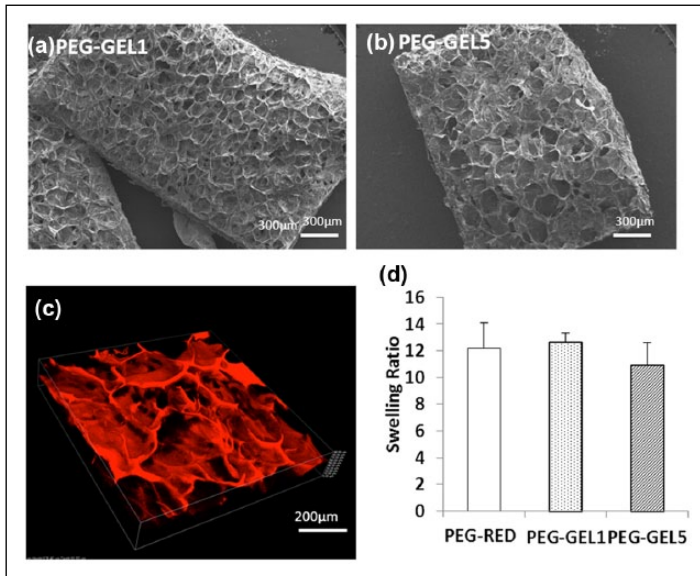


Figure 1. Characterization of 3D macroporous scaffolds. SEM micrographs of (a) PEG-GEL1, (b) PEG-GEL5 revealing porous morphologies with pore diameters ranging between 80 to 200 μm . Scale bar = 300 μm . (c) Homogeneous distribution of gelatin inside PEG-GEL5 scaffolds. Scale bar = 200 μm . (d) Swelling ratio of PEG-GEL1, PEG-GEL5, and PEG-RED as the control group. Data expressed as mean \pm SD, where $n = 3$.

(Figure 4(a)). After 24 h, the loose clusters integrated together to form cell aggregates with average diameters of 50 μm . At Day 3, chondrocytes that had adhered to the PEG-gelatinous networks, flattened out to form elongated morphologies, in comparison with the control group (Figure 4(b)). In addition, the distribution of cell aggregates within the PEG-gelatin scaffolds was also confirmed in Figure 4(c) with chondrocytes (in green) that formed large cell aggregates around gelatinous networks (in red) inside PEG-GEL5 scaffolds (in gray) in culture.

Actin cytoskeleton arrangement in 3D

The arrangement of actin filaments was analyzed at the level of cell attachment to the adhesion surface after Day 3 in culture, using phalloidin-stained F-actin with DAPI (Figure 5(a)). Confocal micrographs revealed robust actin fibers (in red) with varying fiber arrangements across the three experimental groups. The nuclei of cells were stained blue with DAPI. Cells aggregates inside PEG scaffolds displayed rounded morphologies. Notably in PEG-GEL1, cell aggregates in some areas remained rounded with actin fibers firmly surrounding the cells, whereas in some areas, relatively elongated fiber morphologies were observed, suggesting a collaborative effort by cells to retain the natural phenotype of chondrocytes. However, cells cultured in PEG-GEL5 groups developed bundles of stress fibers with elongated and multilateral fiber arrangements. Although the shape of cell aggregates varied in the three experimental groups, however, it was difficult to predict the morphology of individual cells. Additionally, representative Z-stack projections of confocal micrographs (where $n = 5$) were selected to investigate the area of cell aggregates, aspect ratio, and subsequent aggregate roundness. The average values of each category were graphed, respectively (Figure 5(b)–(d)). The area of cell aggregates demonstrated a 22-fold and a 41-fold ($p < 0.05$) increase in PEG-GEL1 and PEG-GEL5 groups, in comparison with PEG-RED (Figure 5(b)). Similarly, the aspect

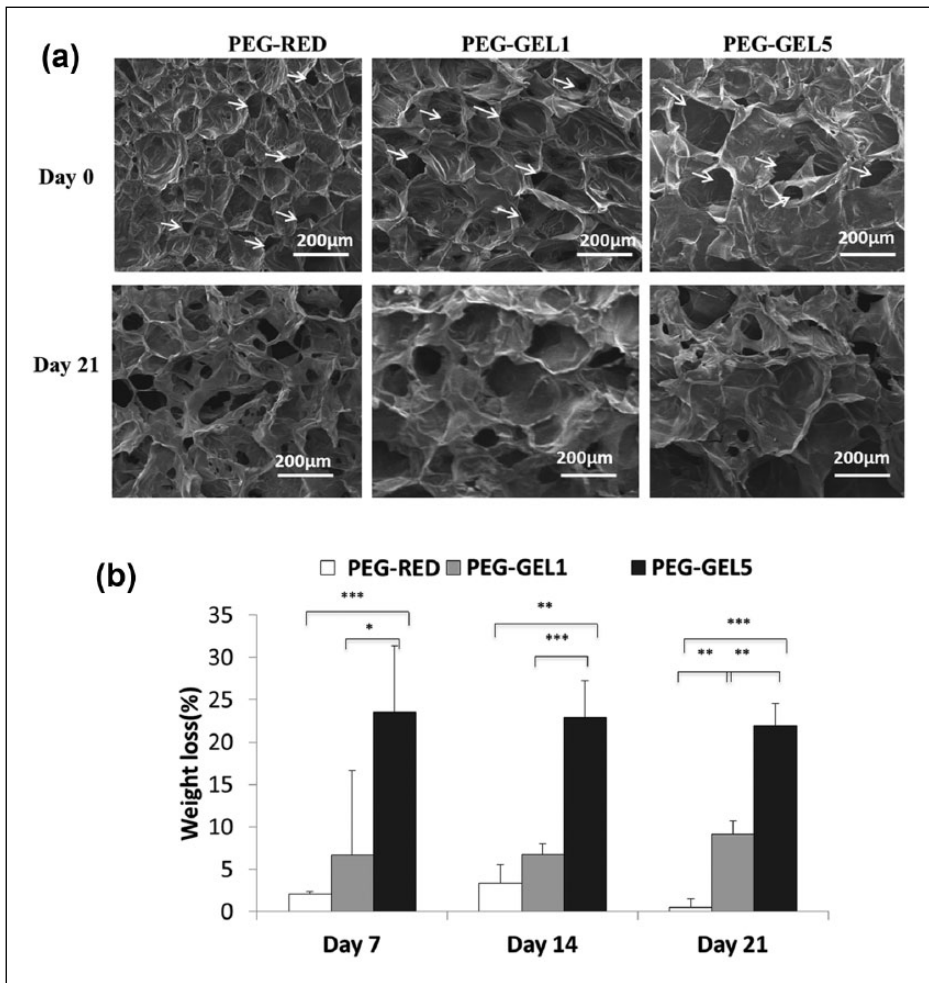


Figure 2. Degradation of macroporous PEG-gelatin scaffolds after 21 days in vitro. (a) SEM micrographs taken at Day 0 and Day 21 of PEG-RED, PEG-GEL1, and PEG-GEL5 scaffolds with average pore diameters of 150 μm. The arrows show the interconnected pore structure within the scaffolds at Day 0. Scale bars = 200 μm. (b) Percentage weight loss after immersion in PBS at Days 7, 14, and 21 in vitro. Data expressed as mean ± SD, where n = 3, *p < 0.05, **p < 0.01, ***p < 0.001.

ratio of cell aggregates was higher in PEG-GEL1 ($p < 0.001$) and PEG-GEL5 ($p < 0.001$), in comparison with the control group (Figure 5(c)). The roundness of cell aggregates was significantly lower in both PEG-GEL1 ($p < 0.001$) and PEG-GEL5 ($p < 0.001$), in comparison with PEG-RED (Figure 5(d)). Statistically, no significant difference in the area of cell aggregates, aspect ratio, and aggregate roundness was found between the groups PEG-GEL1 and PEG-GEL5, respectively.

Integrin $\beta 1$ analysis

Next, to assess the involvement of integrin $\beta 1$ in mediating cell adhesion and cytoskeleton formation in 3D constructs, integrin $\beta 1$ staining and western blotting experiments were conducted after Day 3 in culture (Figure 6). Visually, micrographs displayed increased levels of integrin $\beta 1$ (in

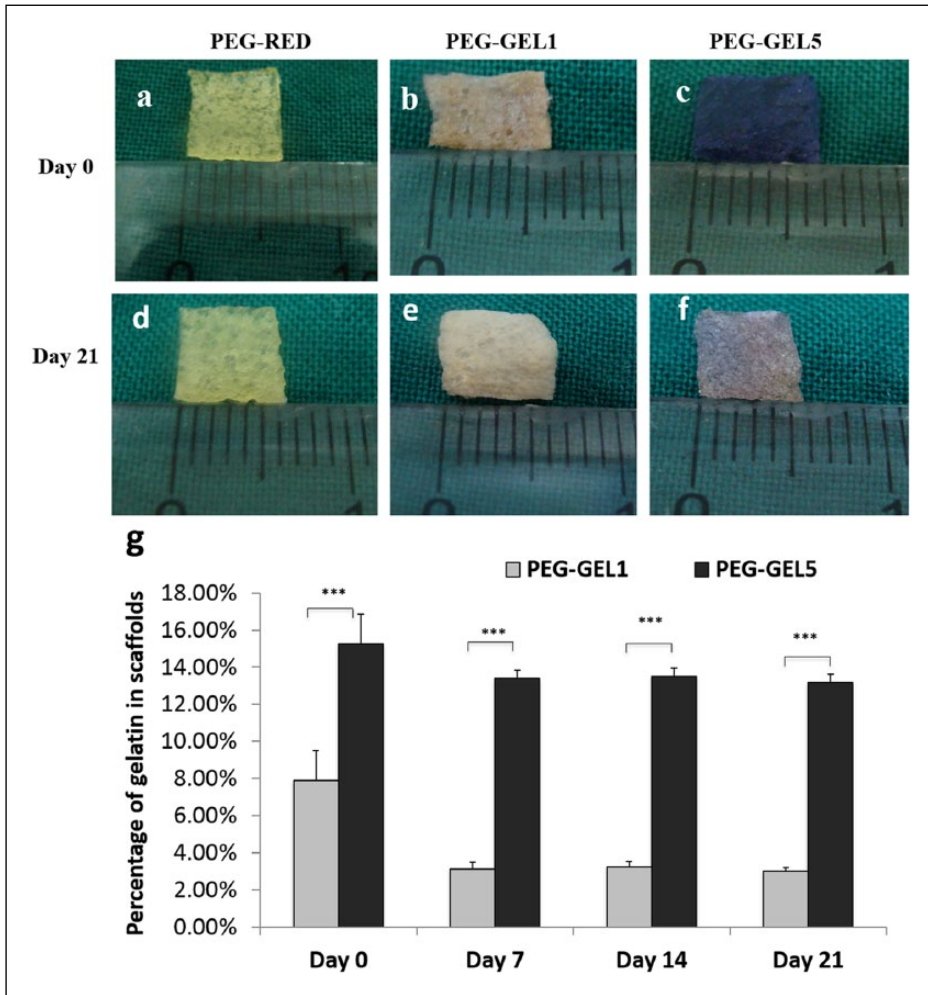


Figure 3. Gelatin remained within scaffolds. Ninhydrin staining of (a, d) PEG-RED, (b, e) PEG-GEL1, and (c, f) PEG-GEL5 at Days 0 and 21. PEG-GEL1 (in pink) and PEG-GEL5 (in purple) were positively stained due to presence of gelatin. Scale bars = 2 mm. (g) Percentage of gelatin (%) remained in macroporous scaffolds after degradation at Days 7, 14, and 21 in vitro. Dry mass of the composite scaffold represents 100% in this calculation. Data expressed as mean \pm SD, where $n = 3$, $^{**}p < 0.01$, $^{***}p < 0.001$.

green) in PEG-GEL5, in comparison with both PEG-RED and PEG-GEL1 (Figure 6(a-i)). Unlike PEG-GEL1 and PEG-GEL5, PEG-RED revealed extremely low levels of integrin $\beta 1$ staining, as expected. Additionally, these findings were further confirmed by western blot analysis, as results indicated that the expression of integrin $\beta 1$ was significantly higher in PEG-GEL5, in comparison to PEG-GEL1 (Figure 6(j)).

Cell proliferation and ECM accumulation in vitro

Interestingly, larger cell aggregates were found in PEG-GEL1 and PEG-GEL5 groups at Days 7 and 14, indicating that cells were actively proliferating within the aggregates (Figure 7(a)). Cell

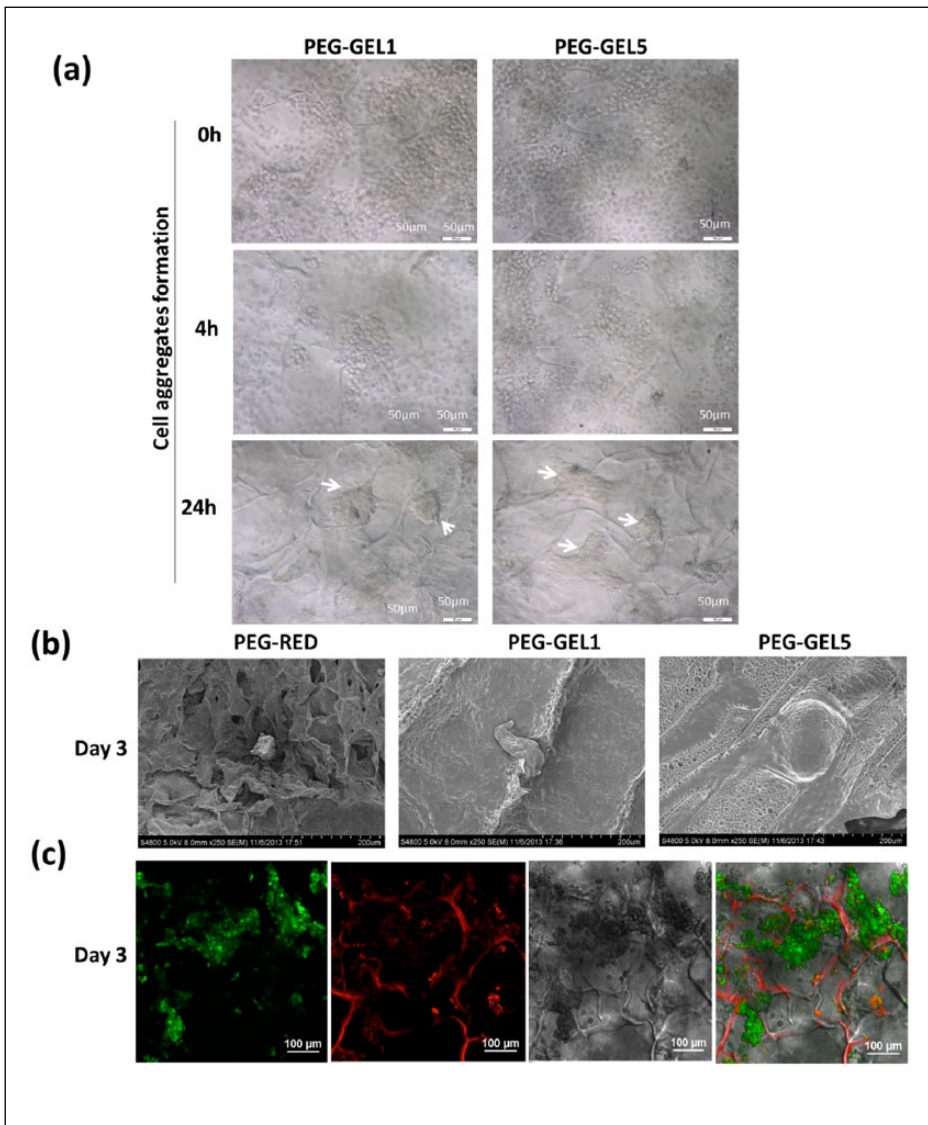


Figure 4. Distribution of chondrocytes within 3D macroporous scaffolds. (a) Cell aggregation in PEG-GEL1 and PEG-GEL5 hydrogels observed at 0, 4, and 24h after initial cell seeding density of 3×10^5 cells/sample. The arrows show cell aggregates within the scaffolds after 24h. Scale bars = 50 μm. (b) SEM micrographs taken at Day 3, with cell aggregates present inside the macroporous scaffolds with varying morphologies. Scale bars = 200 μm (c) Cell distribution inside PEG-GEL5 at Day 3 showing cells (in green), gelatinous networks (in red), and PEG-GEL5 gel-matrix (in gray). Scale bars = 100 μm.

viability was performed using MTT assay. Gelatin incorporation did not affect cell viability at Day 1 and Day 4; however, improved cell viability at Day 7 was observed in PEG-GEL1 and PEG-GEL5 hydrogels (Figure 7(b)). A 2-fold ($p < 0.001$) and a 1.7-fold ($p < 0.01$) increase in viable cell numbers in PEG-GEL1 and PEG-GEL5 groups were recorded, in comparison with the control group (Figure 7(c)). A 1.13-fold ($p < 0.01$) and 1.08-fold ($p < 0.05$) increase in glycosaminoglycan

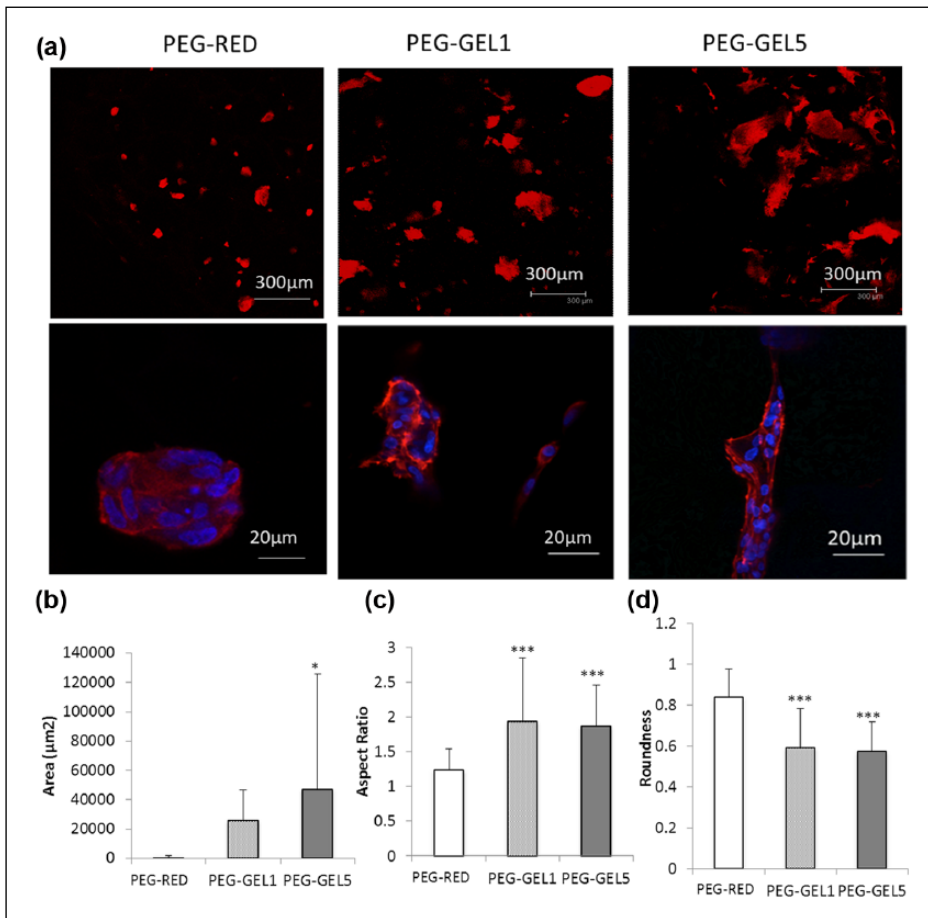


Figure 5. F-actin staining using rhodamine phalloidin with DAPI of chondrocytes embedded in macroporous scaffolds after 3 days in culture. (a) F-actin fibers (in red) surrounding chondrocytes within the enlarged cell aggregates in PEG-RED, PEG-GEL1, and PEG-GEL5. With increase in gelatin composition, F-actin fiber arrangement altered, from a spherical organization following the contour of chondrocytes (as shown in PEG-RED) to a much more multilateral arrangement (as shown in PEG-GEL5). Scale bar = 300 µm. Nuclei of the cells were stained blue with DAPI. Scale bar = 20 µm. Morphology of the cell aggregates was quantified in terms of (b) area (c) aspect ratio, and (d) roundness. Confocal z-stack projections of Alexa Fluor® 546 phalloidin-stained cells were assessed. Error bar represents mean values ± SD, where $n = 5$, * $p < 0.05$; *** $p < 0.001$.

(GAG) production was found inside PEG-GEL1 and PEG-GEL5, in comparison with the control group (Figure 7(d)).

Qualitative real-time PCR

Gene expression of collagen I and II, aggrecan, and Sox-9 were assayed after 14 days in culture by Real-time Polymerase Chain Reaction (RT-PCR). In comparison with PEG-RED, PEG-gelatin scaffolds revealed elevated gene expression of collagen I ($p < 0.001$), collagen II ($p < 0.05$), aggrecan ($p < 0.05$), and sox-9 ($p < 0.01$) in PEG-GEL5 (Figure 8). Overall, a significant 4.8-fold

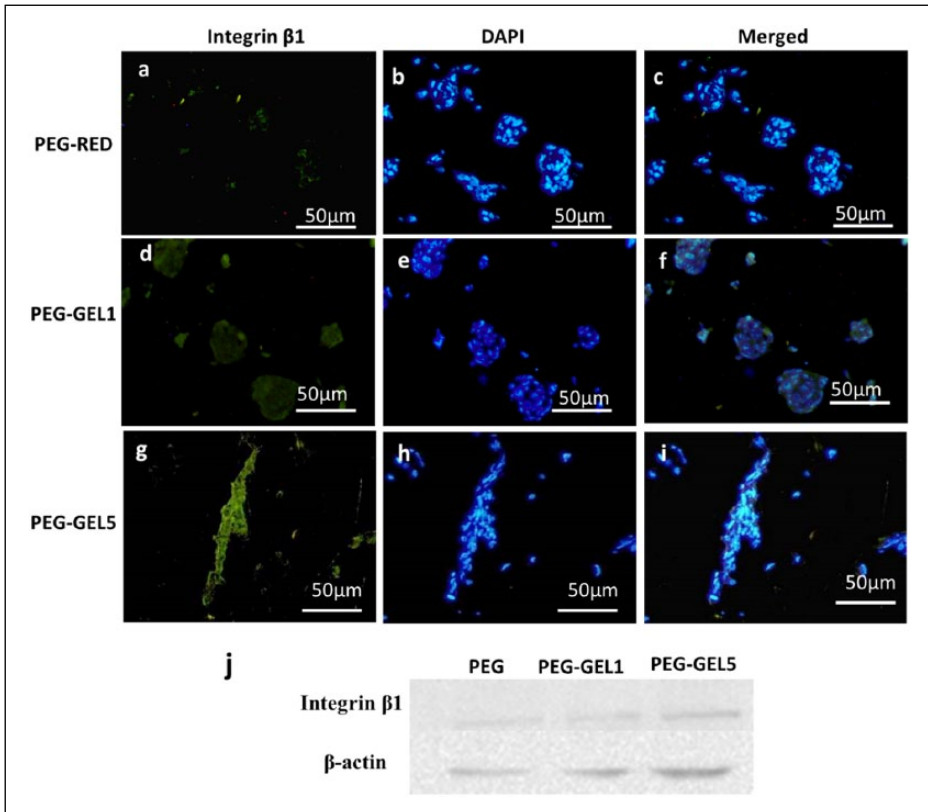


Figure 6. Integrin $\beta 1$ staining of chondrocytes embedded in macroporous scaffolds at Day 3. (a-i) Integrin $\beta 1$ staining (in green) in PEG-GEL1 and PEG-GEL5 in comparison with PEG-RED. Nuclei of the cells were stained blue with DAPI. Scale bars = 50 μm . (j) Western blot analysis of integrin $\beta 1$ expression, with β -actin as the reference.

($p < 0.001$) increase in collagen I and a 2.4-fold ($p < 0.05$) increase in collagen II gene expression were recorded in PEG-GEL5 groups, in comparison with PEG-GEL1 (Figure 8(a)). However, no difference in gene expression of aggrecan and sox-9 was found between PEG-GEL1 and PEG-GEL5 (Figure 8(b)). From these findings, it was evidently clear that chondrocytes in 3D culture deposited collagen II and I simultaneously. Therefore, the ratio of collagen II to collagen I was evaluated via gene expression patterns shown in Figure 8(a). In PEG-GEL1, a significant 12.2-fold higher level of expression of collagen II to collagen I was observed. By contrast, a significant 8.6-fold higher level of expression of collagen II to I was recorded in PEG-GEL5 groups. The experiments were repeated in triplicates to ensure results were accurate and reproducible (where $n = 3$).

Discussion

In this study, two different gradients of gelatin were physically entrapped into macroporous PEG hydrogels to investigate the effect on chondrocyte behavior in vitro. Chondrocytes encapsulated within PEG-GEL1 and PEG-GEL5 groups exhibited improvement in cell adhesion and formed large cell aggregates within 24 h. The concentration of gelatin incorporated into physical blends significantly affected the morphology of chondrocytes, cell proliferation, GAG production, and

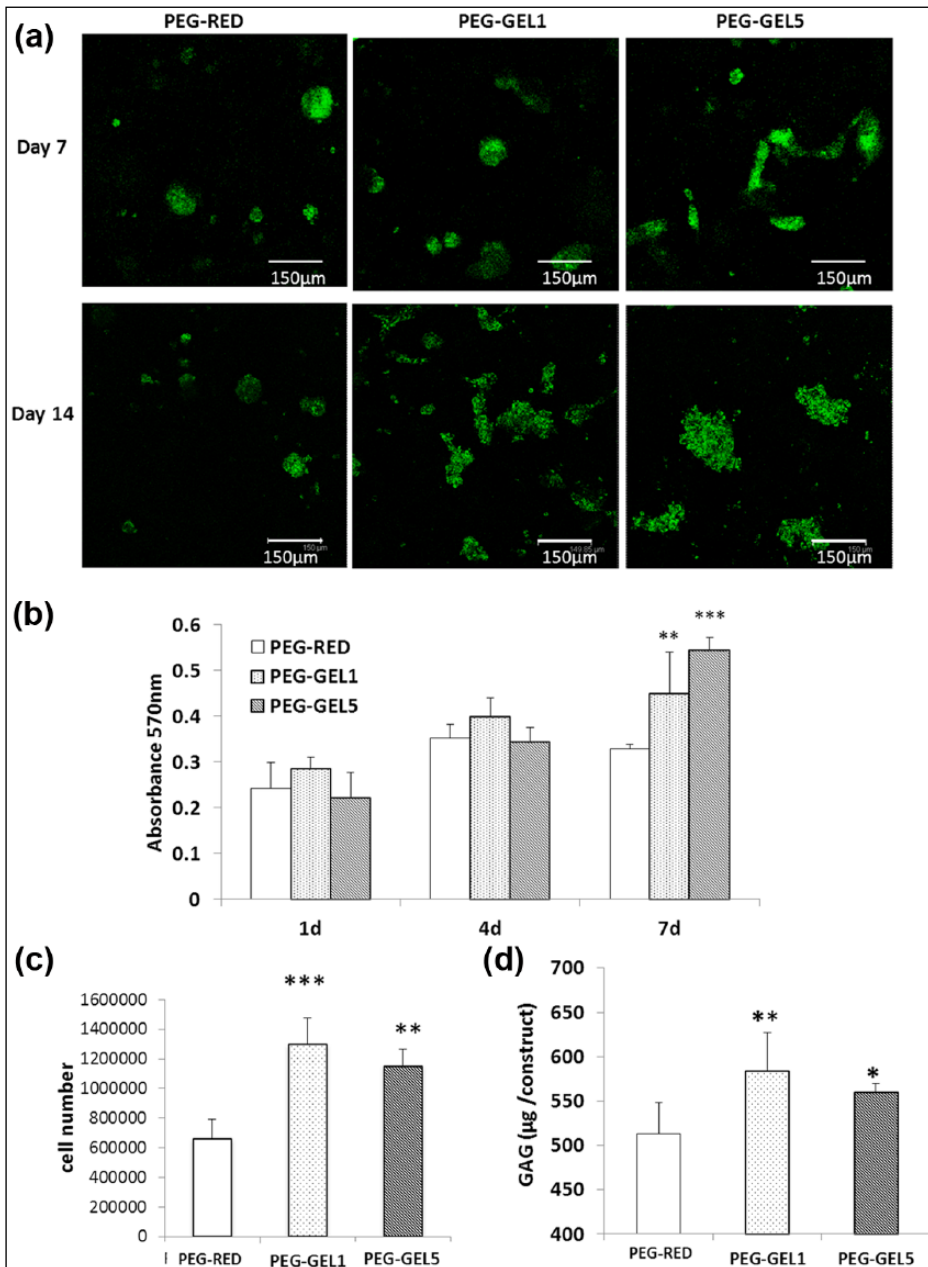


Figure 7. Cell proliferation, cell viability, and GAG accumulation. (a) Cell viability assessed by FDA staining at Days 7 and 14 in culture. PEG-GEL1 and PEG-GEL5 revealed a large number of viable cells (in green) present inside the gel-matrices. Scale bars = 150 µm. (b) MTT assay. Cell viability of PEG-GEL1 and PEG-GEL5 groups compared with PEG-RED group. (c) Quantification of cell number via DNA assay. Cells actively proliferated inside PEG-GEL1 and PEG-GEL5 in comparison with PEG-RED. (d) Total GAG content in all three experimental groups. Elevated levels of GAG content in PEG-GEL1 and PEG-GEL5 were recorded. Data expressed as mean \pm SD, where $n = 3$, * $p < 0.05$; ** $p < 0.01$; *** $p < 0.001$.

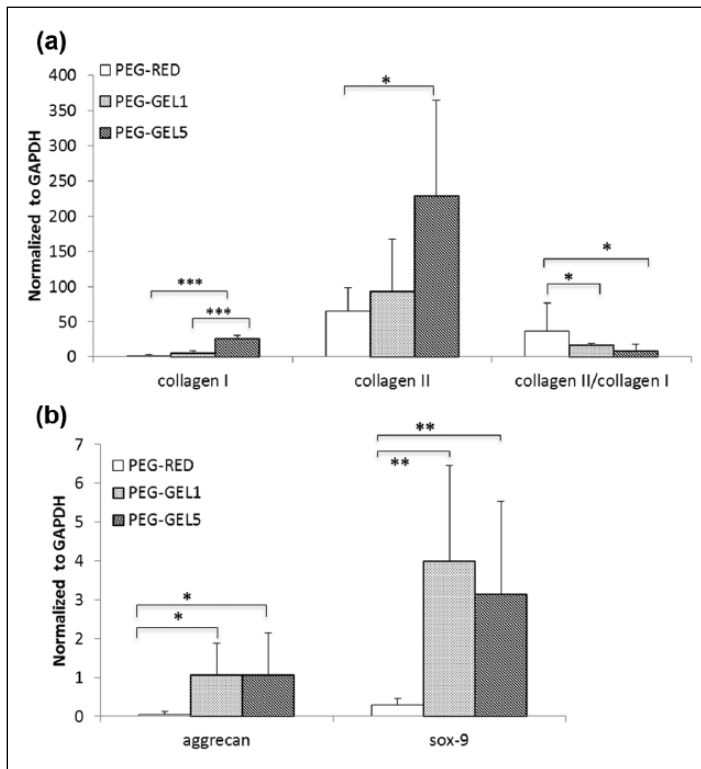


Figure 8. Gene expression levels of collagen I and II, aggrecan, and sox-9 measured at Day 14 in culture. (a) Elevated gene expression levels of collagen I and collagen II and the ratio of collagen II and I (collagen II/collagen I) in PEG-GEL1 and PEG-GEL5 in comparison with PEG-RED. (b) Elevated gene expression levels of aggrecan and sox-9 in PEG-GEL1 and PEG-GEL5 in comparison with PEG-RED. Data expressed as mean \pm SD, where $n = 3$, * $p < 0.05$, ** $p < 0.01$, *** $p < 0.001$.

gene expression. As gelatin is a by-product of collagen hydrolysis, it retains cell-binding domains such as arginine-glycine-aspartic acid (RGD) and matrix metalloproteinase (MMP) sensitive degradation sites that are critical in successful cell adhesion and encapsulation.¹⁴ Therefore, physical blends of PEG-GEL1 and PEG-GEL5 facilitated cell adhesion and enabled the clustering of focal adhesions and the constriction of actin fibers, which in turn strengthened the adhesive forces.²⁷ It was hypothesized that the organization of actin cytoskeleton in an elongated fashion may be a consequence of chondrocyte de-differentiation.²⁸ Under culture conditions, chondrocytes have little proliferative capacity and therefore de-differentiate into fibroblast-like cells to allow cells to re-enter the cell cycle.^{29,30} This transition is further mediated by integrin $\beta 1$. It is well known that elevated expression levels of integrin $\beta 1$ exhibit an increase in cell proliferation. However, blocking integrin $\beta 1$ inhibits cell proliferation.³¹ Chondrocytes that had adhered to both PEG-GEL1 and PEG-GEL5 groups shown by strong integrin $\beta 1$ staining, led to enhanced cell proliferation.

Various gelatin-based scaffolds have been explored for 3D cell encapsulation. Electrospun PCL scaffolds immobilized with 30% gelatin have shown to promote nerve tissue engineering.³² In another study, nanofibrous scaffolds containing 50% gelatin enhanced cell proliferation and differentiation of myoblasts in vitro.³³ Moreover, PCL scaffolds containing gelatin levels as high as

70% were most suitable for chondrocyte culture.¹³ Although the above-mentioned studies were carried out using chemically cross-linked gelatin, however, body of literature clearly suggests that gelatin composition and type of biomaterial can synergistically manipulate cell function.^{12,16} For example, photopolymerized styrenated gelatin hydrogel used for chondrocyte encapsulation maintained viability for up to 21 days in vitro, however, cells did not proliferate within the gel matrix.^{14,34} By contrast, this study demonstrated that macroporous hydrogels containing physically entrapped gelatin (as low as 3%) could not only improve cell viability, but also promoted cell proliferation and GAG biosynthesis for up to 14 days in vitro. The changes in cytoskeleton organization had a predominant effect on GAG synthesis.^{28,35,36} Enhanced gene expression levels of collagen II and aggrecan in both gelatin-modified hydrogels indicate that scaffolds may be capable of facilitating cartilage-like ECM formation. However, further investigation is required to look into cell matrix deposition under long-term culture conditions to validate this design strategy for cartilage engineering applications.

Conclusion

Hitherto, we have shown that minimal entrapment of gelatin can substantially enhance the bioactivity of macroporous PEG hydrogels. Using a cost-effective approach, hydrogel networks of PEG were able to retain gelatin without the use of any cross-linking agent. Resultant scaffolds supported cell viability, proliferation, and GAG synthesis up to 14 days in culture. Elevated gene expressions of cartilage-specific markers such as aggrecan and collagen II indicate the potential application of PEG-gelatin scaffolds for cartilage repair.

Declaration of Conflicting Interests

The author(s) declared no potential conflicts of interest with respect to the research, authorship, and/or publication of this article.

Funding

The author(s) disclosed receipt of the following financial support for the research, authorship, and/or publication of this article: The authors would like to acknowledge support from the National Basic Research Program of China grant (973 Program; 2012CB619100) and the National Natural Science Foundation of China grant (81471800, 81271722).

References

1. McCall JD, Lin CC and Anseth KS. Affinity peptides protect transforming growth factor beta during encapsulation in poly(ethylene glycol) hydrogels. *Biomacromolecules* 2011; 12: 1051–1057.
2. Yang F, Qu X, Cui W, et al. Manufacturing and morphology structure of polylactide-type microtubules orientation-structured scaffolds. *Biomaterials* 2006; 27: 4923–4933.
3. Zhang Y, Choi SW and Xia Y. Modifying the pores of an inverse opal scaffold with chitosan microstructures for truly three-dimensional cell culture. *Macromol Rapid Comm* 2012; 33: 296–301.
4. Kumar G, Tison CK, Chatterjee K, et al. The determination of stem cell fate by 3D scaffold structures through the control of cell shape. *Biomaterials* 2011; 32: 9188–9196.
5. Kim K, Dean D, Wallace J, et al. The influence of stereolithographic scaffold architecture and composition on osteogenic signal expression with rat bone marrow stromal cells. *Biomaterials* 2011; 32(15): 3750–3763.
6. Kim K, Dean D, Lu A, et al. Early osteogenic signal expression of rat bone marrow cells is influenced by both hydroxyapatite nanoparticle contents and initial cell seeding density in biodegradable nanocomposite scaffolds. *Acta Biomater* 2011; 7(3): 1249–1264.

7. Kim K, Yeatts A, Dean D, et al. Stereolithographic bone scaffold parameters: osteogenic differentiation and signal expression. *Tissue Eng Part B Rev* 2010; 16(5): 523–539.
8. Zhao M, Li L, Li X, et al. Three-dimensional honeycomb-patterned chitosan/poly(L-lactic acid) scaffolds with improved mechanical and cell compatibility. *J Biomed Mater Res A* 2011; 98: 434–441.
9. Benoit DS, Schwartz MP, Durney AR, et al. Small functional groups for controlled differentiation of hydrogel-encapsulated human mesenchymal stem cells. *Nat Mater* 2008; 7: 816–823.
10. Lien SM, Ko LY and Huang TJ. Effect of pore size on ECM secretion and cell growth in gelatin scaffold for articular cartilage tissue engineering. *Acta Biomater* 2009; 5: 670–679.
11. Rnjak-Kovacina J, Wray LS, Golinski JM, et al. Arrayed hollow channels in silk-based scaffolds provide functional outcomes for engineering critically sized tissue constructs. *Adv Funct Mater* 2014; 24: 2188–2196.
12. Daniele MA, Adams AA, Naciri J, et al. Interpenetrating networks based on gelatin methacrylamide and PEG formed using concurrent thiol click chemistries for hydrogel tissue engineering scaffolds. *Biomaterials* 2014; 35: 1845–1856.
13. Zheng R, Duan H, Xue J, et al. The influence of Gelatin/PCL ratio and 3-D construct shape of electrospun membranes on cartilage regeneration. *Biomaterials* 2014; 35: 152–164.
14. Fu Y, Kedi X, Zheng X, et al. 3D cell entrapment in crosslinked thiolated gelatin-poly(ethylene glycol) diacrylate hydrogels. *Biomaterials* 2012; 33: 48–58.
15. Hu M, Kurisawa M, Deng R, et al. Cell immobilization in gelatin-hydroxyphenylpropionic acid hydrogel fibers. *Biomaterials* 2009; 30: 3523–3531.
16. Woods A, Couchman JR, Johansson S, et al. Adhesion and cytoskeletal organisation of fibroblasts in response to fibronectin fragments. *EMBO J* 1986; 5: 665–670.
17. Lai JY. Biocompatibility of chemically cross-linked gelatin hydrogels for ophthalmic use. *J Mater Sci Mater Med* 2010; 21: 1899–1911.
18. Vladkova TG. Surface engineered polymeric biomaterials with improved biocontact properties. *Inter J Polym Sci* 2010; 2010: 296094.
19. Lim KS, Alves MH, Poole-Warren LA, et al. Covalent incorporation of non-chemically modified gelatin into degradable PVA-tyramine hydrogels. *Biomaterials* 2013; 34: 7097–7105.
20. Zhu J. Bioactive modification of poly(ethylene glycol) hydrogels for tissue engineering. *Biomaterials* 2010; 31: 4639–4656.
21. Zhang JJ, Yang Z, Li C, et al. Cells behave distinctly within sponges and hydrogels due to differences of internal structure. *Tissue Eng Part A* 2013; 19: 2166–2175.
22. Moon JJ, Hahn MS, Kim I, et al. Micropatterning of poly(ethylene glycol) diacrylate hydrogels with biomolecules to regulate and guide endothelial morphogenesis. *Tissue Eng Part A* 2009; 15: 579–585.
23. Nair S, Remya NS, Remya S, et al. A biodegradable in situ injectable hydrogel based on chitosan and oxidized hyaluronic acid for tissue engineering applications. *Carbohydr Polym* 2011; 85: 838–844.
24. Yang Z, Wu Y, Li C, et al. Improved mesenchymal stem cells attachment and in vitro cartilage tissue formation on chitosan-modified poly(L-lactide-co-epsilon-caprolactone) scaffold. *Tissue Eng Part A* 2012; 18: 242–251.
25. Li C, Wang L, Yang Z, et al. A viscoelastic chitosan-modified three-dimensional porous poly(L-lactide-co-epsilon-caprolactone) scaffold for cartilage tissue engineering. *J Biomater Sci Polym Ed* 2012; 23: 405–424.
26. Simonsson C, Madsen JT, Graneli A, et al. A study of the enhanced sensitizing capacity of a contact allergen in lipid vesicle formulations. *Toxicol Appl Pharmacol* 2011; 252: 221–227.
27. Kambe Y, Takeda Y, Yamamoto K, et al. Effect of RGDS-expressing fibroin dose on initial adhesive force of a single chondrocyte. *Biomed Mater Eng* 2010; 20: 309–316.
28. Purcell BP, Lobb D, Charati MB, et al. Injectable and bioresponsive hydrogels for on-demand matrix metalloproteinase inhibition. *Nat Mater* 2014; 13: 653–661.
29. Margadant C, van Opstal A and Boonstra J. Focal adhesion signaling and actin stress fibers are dispensable for progression through the ongoing cell cycle. *J Cell Sci* 2007; 120: 66–71.
30. Wang HB, Dembo M and Wang YL. Substrate flexibility regulates growth and apoptosis of normal but not transformed cells. *Am J Physiol Cell Physiol* 2000; 279: 1345–1350.

31. Enomoto-Iwamoto M, Iwamoto M, Nakashima K, et al. Involvement of $\alpha 5 \beta 1$ integrin in matrix interactions and proliferation of chondrocytes. *J Bone Miner Res* 1997; 12: 1124–1132.
32. Ghasemi-Mobarakeh L, Prabhakaran MP, Morshed M, et al. Electrospun poly(epsilon-caprolactone)/gelatin nanofibrous scaffolds for nerve tissue engineering. *Biomaterials* 2008; 29: 4532–4539.
33. Kim MS, Jun I, Shin YM, et al. The development of genipin-crosslinked poly(caprolactone) (PCL)/gelatin nanofibers for tissue engineering applications. *Macromol Biosci* 2010; 10: 91–100.
34. Hoshikawa A, Nakayama Y, Matsuda T, et al. Encapsulation of chondrocytes in photopolymerizable styrenated gelatin for cartilage tissue engineering. *Tissue Eng* 2006; 12: 2333–2341.
35. Schuh E, Hofmann S, Stok K, et al. Chondrocyte redifferentiation in 3D: the effect of adhesion site density and substrate elasticity. *J Biomed Mater Res A* 2012; 100: 38–47.
36. Moreira Teixeira LS, Leijten JCH, Sobral J, et al. High throughput generated micro-aggregates of chondrocytes stimulated cartilage formation in vitro and in vivo. *Eur Cell Mater* 2012; 23: 387–399.